Quantum interference of electromagnetic fields from remote quantum memories

T. Chanelière, D. N. Matsukevich, S. D. Jenkins, S.-Y. Lan, R. Zhao, T. A. B. Kennedy, and A. Kuzmich
School of Physics, Georgia Institute of Technology, Atlanta, Georgia 30332-0430
(Dated: February 1, 2008)

We observe quantum, Hong-Ou-Mandel, interference of fields produced by two remote atomic memories. High-visibility interference is obtained by utilizing the finite atomic memory time in four-photon delayed coincidence measurements. Interference of fields from remote atomic memories is a crucial element in protocols for scalable generation of multi-node remote qubit entanglement.

PACS numbers: 42.50.Dv,03.65.Ud,03.67.Mn

Proposed approaches to scalable quantum information networks and distributed quantum computing involve linear optical elements and single-photon detectors [1, 2, 3]. Photoelectric detection events signal entanglement creation and, by postselection, eliminate undesirable components of the electromagnetic field. While postselection has a residual negative effect on the scaling of the overall efficiency of quantum information protocols, this can be offset by quantum memory, a resource which provides the capability to perform quantum state transfer from matter to light and vice versa, as demonstrated with cold atomic ensembles [4, 5, 6]. These also act as sources of entangled photon pairs, with quantum memory enabling user-controlled delays between the photons.

In order to distribute entanglement over a network configuration we must connect entangled elements at remote sites. This may be achieved by interfering photons, produced at these sites, on a beamsplitter followed by coincident photoelectric detection. The anticorrelation of coincidence counts is the signature of Hong-Ou-Mandel interference (HOM), whereby single photons simultaneously incident at two input ports of a beamsplitter both exit in one or other of the output ports [7, 8]. For distinct, remote quantum memory elements, HOM is a possible method for entanglement connection operations that scale efficiently with the number of elements. Several remarkable demonstrations of HOM using parametric down-conversion (PDC) have been reported (see Refs. [8, 9, 10] and references therein). It has also been observed using photon pairs generated locally by a single source - a quantum dot [11], an atom [12], and an atomic ensemble [13]. Recently HOM has been demonstrated with two (a) neutral atoms [14] and (b) ions [15], in each case separated by a few microns.

In this Letter we report HOM from remote sources (cold atomic ensembles) with quantum memory, located in adjacent laboratories and separated by 5.5 m (Fig. 1). In a particular ensemble signal photons are generated by Raman scattering of a write laser pulse with temporal profile $\varphi(t)$ (normalized to unity $\int dt\ |\varphi(t)|^2 = 1$), whose length is much greater than the ensemble dimensions. For an unpolarized ensemble of N atoms interacting with an off-resonant vertically ($\mathbf{e}_V = -\hat{\mathbf{z}}$) polarized write field propagating in the y-direction, the interaction picture

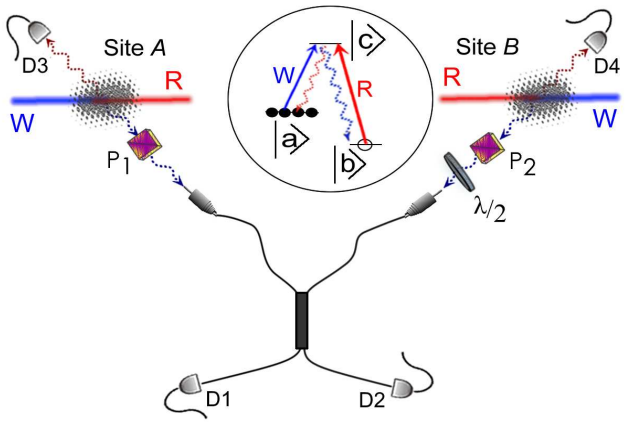

FIG. 1: Schematic showing Raman scattering of write pulses (W) at sites A and B with signal fields collected by polarizers P_1 and P_2 and optical fiber beamsplitter and directed towards detectors D1, D2. A half-wave plate ($\lambda/2$) may be inserted at site B to rotate light polarization. Raman scattering of delayed read pulses produces idler fields detected at D3, D4. The inset shows the atomic level structure and the write- and read-induced Raman processes.

Hamiltonian for the system includes a term representing Raman scattering into the detected signal mode defined by an optical fiber, and described by [16]

$$\hat{H}(t) = i\hbar\chi\varphi(t)\left(\cos\eta\ \hat{\psi}_H^\dagger(t)\,\hat{s}_H^\dagger + \sin\eta\ \hat{\psi}_V^\dagger(t)\,\hat{s}_V^\dagger\right) + h.c. \quad (1)$$

The annihilation operator for the Raman scattered field emitted from the ensemble is given by $\hat{\psi}_\lambda(t)$, $\lambda = H, V$. These field operators obey the usual free-field, narrow bandwidth bosonic commutation relations $\left[\hat{\psi}_\lambda(t), \hat{\psi}_{\lambda'}^\dagger(t')\right] = \delta_{\lambda,\lambda'}\delta(t-t')$. The emission of H- or V-polarized signal photons creates correlated atomic spin wave excitations with annihilation operators $\hat{s}_{H,V}$ given by, $\hat{s}_V = -\hat{s}_0$, and

$$\hat{s}_H = \cos\theta\hat{s}_{-1} - \sin\theta\hat{s}_{+1}, \quad (2)$$

where $\cos^2\theta = \sum_m p_m X_{m,-1}^2 / \sum_{\alpha=\pm1}\sum_m p_m X_{m,\alpha}^2$ and

the spherical vector components of the spin wave are given by

$$\hat{s}_\alpha \equiv \sum_{m=-F_a}^{F_a} \frac{\sqrt{p_m} X_{m,\alpha}}{\sqrt{\sum_m p_m |X_{m,\alpha}|^2}} \hat{s}_{m,\alpha}.$$

An atom is prepared in the state $|a,m\rangle$ with probability $p_m = 1/(2F_a+1)$ for an unpolarized ensemble. Here $|a\rangle$ and $|b\rangle$ are the ground hyperfine levels and $|c\rangle$ is the excited level associated with the D_1-line involved in the Raman process, with total angular momenta F_a, F_b and F_c, respectively, and $X_{m,\alpha} \equiv C^{F_a\ 1\ F_c}_{m\ 0\ m} C^{F_b\ 1\ F_c}_{m-\alpha\ \alpha\ m}$ is a product of Clebsch-Gordan coefficients. The spin wave is defined in terms of the μ-th atom transition operators $\tilde{\sigma}^{\mu}_{a,m;\ b,m'}(t)$ and the write $\phi_w(\mathbf{r})$ and signal $\phi_s(\mathbf{r})$ mode spatial profiles (normalized to unity in their respective transverse planes)

$$\hat{s}_{m,\alpha} \equiv \frac{i\bar{A}}{\sqrt{p_m N}} \sum_{\mu=1}^{N} \tilde{\sigma}^{\mu}_{a,m;\ b,m-\alpha}(t) e^{i(\mathbf{k}_s - \mathbf{k}_w)\cdot\mathbf{r}_\mu} \phi_s(\mathbf{r}_\mu) \phi_w^*(\mathbf{r}_\mu), \tag{3}$$

where $\mathbf{k}_s$ and $\mathbf{k}_w$ are the detected signal and write beam wavevectors, respectively, and $\bar{A}$ is the effective overlap area of the write beam and the detected signal mode [16, 17].

The dimensionless parametric coupling constant χ is given by

$$\chi \equiv \frac{2 d_{cb} d_{ca}}{\Delta} \frac{\sqrt{k_s k_w n_w N}}{\hbar \epsilon_0 \bar{A}} \sqrt{\sum_m p_m (X^2_{m,0} + \sum_{\alpha=\pm1} X^2_{m,\alpha}/2)}, \tag{4}$$

where $\Delta = c k_w - (\omega_c - \omega_a)$ is the write laser detuning from the $c \leftrightarrow a$ transition, d_{cb} and d_{ca} are reduced dipole matrix elements for the $c \leftrightarrow b$ and $c \leftrightarrow a$ transitions, n_w is the average number of photons in the write pulse, and the parametric mixing angle η is given by [5, 16]

$$\cos^2\eta = \frac{\frac{1}{2}\sum_{\alpha=\pm1}\sum_m p_m X^2_{m,\alpha}}{\sum_m p_m X^2_{m,0} + \frac{1}{2}\sum_{\alpha=\pm1}\sum_m p_m X^2_{m,\alpha}}. \tag{5}$$

The interaction picture Hamiltonian also includes terms representing Rayleigh scattering, as well as the Raman scattering into undetected modes. One can show however that these commute with the signal Hamiltonian to order $O\left(1/\sqrt{N}\right)$ and that they commute with $\hat{\psi}_\lambda$ and $\hat{s}_\alpha$. As a result, the interaction picture density operator for the signal-spin wave system (tracing over uncollected modes) is given by $\hat{\rho} = \hat{U}\hat{\rho}_0\hat{U}^\dagger$, where $\hat{\rho}_0$ is the initial state of the unpolarized ensemble and vacuum electromagnetic field and the unitary operator $\hat{U}$ is given by

$$\hat{U} = \exp\left(\chi \cos\eta \hat{a}^\dagger_H \hat{s}^\dagger_H + \chi \sin\eta \hat{a}^\dagger_V \hat{s}^\dagger_V - h.c.\right) \tag{6}$$

with the discrete signal mode bosonic operator $\hat{a}_\lambda \equiv \int dt\ \varphi^*(t)\,\hat{\psi}_\lambda(t)$, where $\lambda = H$ or V. In effect the multi-mode, multi-particle system reduces to a discrete mode parametric interaction.

Since $\hat{a}_\lambda$ commutes with the Rayleigh scattering and undetected Raman scattering Hamiltonians, the Heisenberg picture solutions are given by

$$\begin{aligned}\hat{a}^{(out)}_H &= \hat{U}^\dagger \hat{a}^{(in)}_H \hat{U} \\ &= \cosh(\chi\cos\eta)\ \hat{a}^{(in)}_H + \sinh(\chi\cos\eta)\,\hat{s}^{(in)\dagger}_H,\end{aligned}$$

$$\begin{aligned}\hat{a}^{(out)}_V &= \hat{U}^\dagger \hat{a}^{(in)}_V \hat{U} \\ &= \cosh(\chi\sin\eta)\ \hat{a}^{(in)}_V + \sinh(\chi\sin\eta)\,\hat{s}^{(in)\dagger}_V.\end{aligned}$$

These solutions allow calculation of the photoelectric detection signal for an atomic quantum memory element. In this work, two magneto-optical traps (MOTs) of ^{85}Rb, A and B, located in adjacent laboratories, serve as the basis for distant quantum memories (Fig.1). The corresponding Raman scattered signal field operator for the detected mode with spatiotemporal mode $\varphi_{A[B]}(t - z_{A[B]}/c)$ is given by

$$\hat{E}^{(+)}_{\lambda,A} = \sqrt{\frac{\hbar k_s}{2\epsilon_0}} e^{-ick_s\left(t - \frac{z_A}{c}\right)} \phi_{s,A}(\mathbf{r})\, \varphi_A\left(t - \frac{z_A}{c}\right) \hat{a}^{(out)}_{\lambda,A},$$

with a similar expression for ensemble B.

The fields from A and B are combined on a beamsplitter $R + T = 1$, where R and T are its reflectance and transmittance, and the fields $\hat{E}_{\lambda,1}$, $\hat{E}_{\lambda,2}$ in the output ports 1 and 2 are incident on detectors D1 and D2, respectively. We employ vertically (V) polarized write beams, derived from the same laser, and detect the horizontally (H) polarized signal fields, which are passed through polarizing cubes prior to the beamsplitter.

The corresponding cross-correlation function $G^{(12)}_\parallel(t, t+\tau) \equiv \langle \hat{E}^-_{H,1}(t)\hat{E}^-_{H,2}(t+\tau)\hat{E}^+_{H,2}(t+\tau)\hat{E}^+_{H,1}(t)\rangle$ exhibits the HOM effect:

$$\begin{aligned} &G^{(12)}_\parallel(t, t+\tau) = \\ &\mathcal{E}^2_A \mathcal{E}^2_B |T\varphi_A(t+\tau)\varphi_B(t) - R\varphi_B(t+\tau)\varphi_A(t)|^2 s^2_A s^2_B \\ +\ &2RT\left(\mathcal{E}^4_A |\varphi_A(t+\tau)\varphi_A(t)|^2 s^4_A + \mathcal{E}^4_B |\varphi_B(t+\tau)\varphi_B(t)|^2 s^4_B\right)\end{aligned} \tag{7}$$

where $s_{A[B]} \equiv \sinh(\chi_{A[B]}\cos\eta)$, and $\mathcal{E}_{A[B]} = \sqrt{\hbar c k_s/(2\epsilon_0)}|\phi_{s,A[B]}(\mathbf{r})|$. The first, HOM, term on the right-hand side of Eq.(7) exhibits two photon interference and can be understood in terms of conventional single-photon interference conditioned on the first photoelectric detection at time t [12]. For zero delay $\tau = 0$ and a symmetric beamsplitter $R = T = 1/2$, this term gives zero contribution even for $\varphi_A \neq \varphi_B$. Alternatively, for $\varphi_A = \varphi_B$ it vanishes for arbitrary τ. However, $G^{(12)}_\parallel(t, t+\tau)$ does not vanish completely due to contributions from multiphoton signal excitations (second term in Eq. (7)). To quantify the degree of the HOM effect, the following benchmark measurement is performed. We

insert a half-wave plate into the path of the signal field from ensemble B, rotating its polarization from H to V, thus nullifying the HOM effect. Quantitatively, in this case the corresponding correlation function $G_{\perp}^{(12)}(t,t+\tau)$ is given by Eq.(7), but now without the interference contributions (proportional to the product RT) in the HOM term.

In our experiment magneto-optical traps (MOTs) of ^{85}Rb are used to provide optically thick atomic ensembles at sites A and B (Fig.1). The ground levels $\{|a\rangle;|b\rangle\}$ correspond to the $5S_{1/2}, F=\{3,2\}$ levels of ^{85}Rb, and the excited level $|c\rangle$ represents the $\{5P_{1/2}, F=3\}$ level of the D_1 line at 795 nm. For a linearly polarized write field we observe that the signal field is nearly orthogonally polarized, consistent with the theoretical value of $\cos^2\eta = 91/122$, Eq.(5).

In order to generate indistinguishable signal wavepackets from the two atomic memories, we produce their respective *write* fields by splitting a single pulse and directing the outputs into identical 100 m long optical fibers. The two Raman-scattered signal fields produced at A and B are passed through polarizing cubes to select the H-components and coupled into the ends of a fiber-based beam splitter. The outputs of the latter are connected to single-photon counting modules D1 and D2. A half-wave plate is inserted into the path of signal field B (Fig. 1) which allows us to vary the relative (linear) polarization of the detected fields. This allows us to detect parallel polarizations ($||$), which exhibit the HOM effect, and orthogonal polarizations ($\perp$), which do not.

Particular care is taken to eliminate possible sources of spectral broadening. Magnetic trapping fields are switched off after atomic collection and cooling, and the residual ambient field is compensated by sets of Helmholtz coils. All trapping and cooling light fields are switched off during data acquisition. The trapping light is shut off about 10 μs before the repumping light, preparing unpolarized atoms in level $|a\rangle$.

In Fig. 2 we show the measured ratio of the photoelectric coincidence rates $\mathcal{R}_{\|}/\mathcal{R}_{\perp}$, which are integrated over the duration of the write pulses. Our measurements exclude Rayleigh scattering on the *write* transition by means of frequency filtering. The experimental ratio $\mathcal{R}_{\|}/\mathcal{R}_{\perp}$ is compared to the ratio of integrated correlation functions $\int\int dtd\tau G_{\|}^{(12)}(t,t+\tau)$ and $\int\int dtd\tau G_{\perp}^{(12)}(t,t+\tau)$, assuming identical wavepackets $\varphi_A=\varphi_B$. We observe scatter in the data beyond the deviations due to photoelectron counting statistics. These indicate the level of systematic drifts encountered over several hours of data acquisition.

The photoelectric coincidences arise from the signal field excitation pairs produced (I) one excitation from each ensemble; (II) both excitations from ensemble A; (III) both excitations from ensemble B. The HOM visibility of $V\equiv 1-\mathcal{R}_{\|}/\mathcal{R}_{\perp}=1/3$ reflects the deleterious

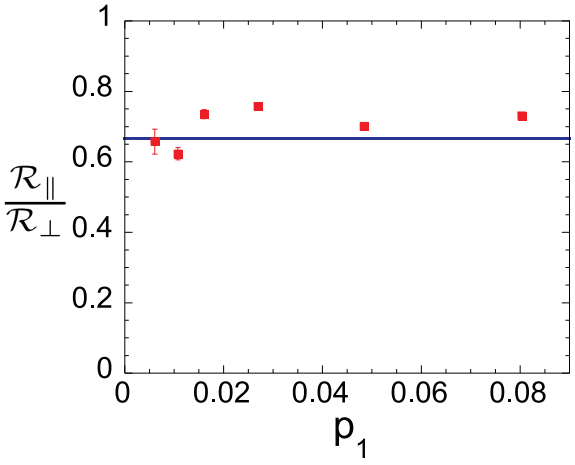

FIG. 2: Ratio of measured two-fold coincidence rates for the $\perp$ and $\|$ configurations). The parameter $p_1\equiv(N_1+N_2)/N_T$ (averaged over the $\perp$ and $\|$ cases). Here $N_1(N_2)$ is the number of photoelectric detections in detector $D1(D2)$, N_T is the number of experimental trials. Theoretically it can be expressed as $p_1=\epsilon_A s_A^2+\epsilon_B s_B^2$, where $\epsilon_A(\epsilon_B)\approx 0.05-0.07$ is the overall probability to detect a signal photon from site A (site B) by either D1 or D2. Scatter beyond the estimated Poissonian level of uncertainty is consistent with systematic drifts in experimental conditions, in particular the single count rates from each ensemble. The solid line is our theoretical prediction based on Eq.(7), for $R=T=1/2$ and $\epsilon_A s_A^2=\epsilon_B s_B^2$.

effects of contributions (II) and (III). These are relatively large because in the limit of weak excitation the spin wave-signal state is dominated by the vacuum contribution. By detecting the presence of a spin wave atomic excitation in each ensemble, these contributions could be substantially suppressed, and the HOM visibility $V\to 1$ in the limit that the excitation probability $p_1\to 0$.

We obtain high-visibility HOM fringes by means of a four-photon delayed coincidence detection procedure. This involves conversion of the spin wave excitation to an idler field by means of an incident read laser pulse which follows the write pulse by a programmable time delay δt in the off-axis geometry [18]; δt is limited by the quantum memory coherence time τ_c [19]. By careful minimization of ambient magnetic fields, $\tau_c>30$ μs have been reported [20]. In this work we choose $\delta t=100$ ns in order to maximize the repetition rate of the protocol. The four-fold detection of the two idler and two signal fields involves HOM of the two signal fields and delayed coincidence detection of the idler fields at detectors D3 and D4, as shown in Fig. 1.

The four-fold coincidence rate is thus given by

$$\mathcal{R}_{\|}^{(4)} \sim s_A^2 s_B^2\left\{(R-T)^2(1+2s_A^2)(1+2s_B^2) + 2RT\left(3s_A^4+3s_B^4+2s_A^2+2s_B^2\right)\right\}. \quad (8)$$

We have again assumed identical wavepacket modes for both ensembles.

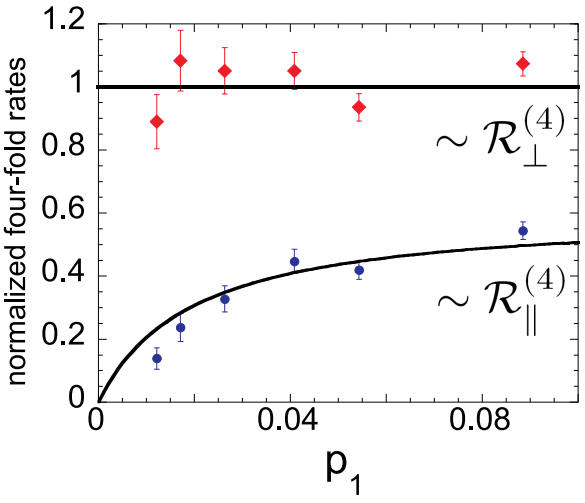

FIG. 3: Integrated four-fold coincidence rates $\mathcal{R}_{\parallel}^{(4)}/\mathcal{W}_{\perp}^{(4)}$ and $\mathcal{R}_{\perp}^{(4)}/\mathcal{W}_{\perp}^{(4)}$ as a function of p_1. Experiment, dots, theory, solid line, assuming identical signal mode wavepackets from each ensemble. Uncertainties are based on the statistics of the photon counting events.

By inserting a half-wave plate into the path of the signal field from ensemble B as before (rotating polarization from H to V), we suppress the HOM interference contributions, such that the four-fold coincidence rate becomes

$$\begin{aligned}\mathcal{R}_{\perp}^{(4)} &\sim s_A^2 s_B^2 \left\{(R^2+T^2)(1+2s_A^2)(1+2s_B^2)\right. \\ &+ \left. 2RT\left(3s_A^4+3s_B^4+2s_A^2+2s_B^2\right)\right\}. \qquad (9)\end{aligned}$$

In separate sets of measurements we recorded photoelectric events with one, or other, of the two MOTs blocked, which allow us to determine the expected level of four-fold coincidences for orthogonal polarizations of the two signal fields $\mathcal{W}_{\perp}^{(4)}$ (i.e., in the absence of HOM). In Fig. 3 we plot $\mathcal{R}_{\parallel}^{(4)}/\mathcal{W}_{\perp}^{(4)}$ and $\mathcal{R}_{\perp}^{(4)}/\mathcal{W}_{\perp}^{(4)}$ along with the corresponding theoretical predictions. HOM interference is manifested in that $\mathcal{R}_{\parallel}^{(4)}/\mathcal{W}_{\perp}^{(4)} \to 0$ as $p_1 \to 0$. The highest observed visibility $V \equiv 1 - \mathcal{R}_{\parallel}^{(4)}/\mathcal{W}_{\perp}^{(4)} \approx 0.86 \pm 0.03$. As the theory and the experimental data agree within the statistical uncertainties, this indicates very good wave-packet overlap of the signals produced by the remote ensembles.

In conclusion, we have demonstrated quantum interference of electromagnetic fields emitted by remote quantum memory elements separated by 5.5 m. Such high-visibility interference is an important element towards scalable distributed entanglement, the central resource in proposed quantum network and distributed quantum computing systems [1, 21, 22, 23, 24, 25].

We gratefully acknowledge illuminating discussions with M. S. Chapman. This work was supported by NSF, ONR, NASA, Alfred P. Sloan and Cullen-Peck Foundations.

[1] E. Knill, R. Laflamme, and G. J. Milburn, Nature (London) **409**, 46 (2001).
[2] L.-M. Duan *et al.*, Nature (London) **414**, 413 (2001).
[3] T. Chanelière *et al.*, Phys. Rev. Lett. **96**, 093604 (2006).
[4] D. N. Matsukevich and A. Kuzmich, Science **306**, 663 (2004); similar results were reported a year later in C. W. Chou *et al.*, Nature (London), **438**, 828 (2005).
[5] D. N. Matsukevich *et al.*, Phys. Rev. Lett. **95**, 040405 (2005); similar results were reported a year later in H. de Riedmatten *et al.*, Phys. Rev. Lett. **97**, 113603 (2006).
[6] D. N. Matsukevich *et al.*, Phys. Rev. Lett. **96**, 030405 (2006).
[7] C. K. Hong, Z. Y. Ou, and L. Mandel, Phys. Rev. Lett. **59**, 2044 (1987).
[8] L. Mandel and E. Wolf, *Optical Coherence and Quantum Optics*, (Cambridge University Press, 1995).
[9] L. Mandel, Rev. Mod. Phys. **71**, S274 (1999).
[10] A. Zeilinger, Rev. Mod. Phys. **71**, S288 (1999).
[11] C. Santori *et al.*, Nature (London) **419**, 594 (2002).
[12] T. Legero, T. Wilk, M. Hennrich, G. Rempe, and A. Kuhn, Phys. Rev. Lett. **93**, 070503 (2004).
[13] J. Thompson *et al.*, Science **313**, 74 (2006).
[14] J. Beugnon *et al.*, Nature (London) **440**, 779 (2006).
[15] P. Maunz *et al.*, quant-ph/0608047.
[16] S. D. Jenkins, Ph. D. Dissertation, Georgia Institute of Technology (2006).
[17] A. Kuzmich and T. A. B. Kennedy, Phys. Rev. Lett. **92**, 030407 (2004).
[18] V. Balic *et al.*, Phys. Rev. Lett. **94**, 183601 (2005).
[19] T. Chanelière *et al.*, Nature (London) **438**, 833 (2005).
[20] D. N. Matsukevich *et al.*, Phys. Rev. Lett. **97**, 013601 (2006).
[21] H. J. Briegel, W. Duer, J. I. Cirac, and P. Zoller, Phys. Rev. Lett. **81**, 5932 (1998).
[22] H. J. Briegel and R. Raussendorf, Phys. Rev. Lett. **86**, 910 (2001).
[23] Y. L. Lim, A. Beige, and L. C. Kwek, Phys. Rev. Lett. **95**, 030505 (2005).
[24] Y. L. Lim *et al.*, Phys. Rev. **73**, 012304 (2006).
[25] D. E. Browne and T. Rudolph, Phys. Rev. Lett. **95**, 010501 (2005).